Drosophila Inducer of MEiosis 4 (IME4) is required for Notch signaling during oogenesis

Cintia F. Hongay[a] and Terry L. Orr-Weaver[a,b,1]

[a]Whitehead Institute for Biomedical Research and [b]Department of Biology, Massachusetts Institute of Technology, Cambridge, MA 02142

Contributed by Terry L. Orr-Weaver, July 18, 2011 (sent for review May 27, 2011)

N^6-methyladenosine is a nonediting RNA modification found in mRNA of all eukaryotes, from yeast to humans. Although the functional significance of N^6-methyladenosine is unknown, the *Inducer of MEiosis 4* (*IME4*) gene of *Saccharomyces cerevisiae*, which encodes the enzyme that catalyzes this modification, is required for gametogenesis. Here we find that the *Drosophila IME4* homolog, *Dm ime4*, is expressed in ovaries and testes, indicating an evolutionarily conserved function for this enzyme in gametogenesis. In contrast to yeast, but as in *Arabidopsis*, *Dm ime4* is essential for viability. Lethality is rescued fully by a wild-type transgenic copy of *Dm ime4* but not by introducing mutations shown to abrogate the catalytic activity of yeast Ime4, indicating functional conservation of the catalytic domain. The phenotypes of hypomorphic alleles of *Dm ime4* that allow recovery of viable adults reveal critical functions for this gene in oogenesis. Ovarioles from *Dm ime4* mutants have fused egg chambers with follicle-cell defects similar to those observed when Notch signaling is defective. Indeed, using a reporter for Notch activation, we find markedly reduced levels of Notch signaling in follicle cells of *Dm ime4* mutants. This phenotype of *Dm ime4* mutants is rescued by inducing expression of a constitutively activated form of Notch. Our study reveals the function of IME4 in a metazoan. In yeast, this enzyme is responsible for a crucial developmental decision, whereas in *Drosophila* it appears to target the conserved Notch signaling pathway, which regulates many vital aspects of metazoan development.

cell fate specification | meiosis | mRNA methylation | oocyte

N^6-methyladenosine (N^6-mA) is a modification found in less than 2% of all adenosines of eukaryotic pools of messenger RNA (1). Unlike other modifications, it does not change the identity of the base it modifies, and thus its presence cannot be inferred from the cDNA sequence. The existence of N^6-mA in eukaryotic mRNA has been known for 4 decades, but its biological function has been elusive (2). However, the enzyme responsible for this modification is present, with very few exceptions, in all eukaryotes, implying a biological function for the N^6-mA–modified mRNA species that has been kept throughout evolution.

Inducer of MEiosis 4 (*IME4*), the gene encoding N6-methyladenosine transferase in *Saccharomyces cerevisiae*, is required for entry into meiosis. It is expressed in mating-type locus a/mating-type locus α diploid cells and is required for mRNA accumulation of *IME1*, the transcription factor known to be the master regulator of yeast meiosis (3). Ectopic expression of *IME4* in haploids is sufficient for these cells to initiate the meiotic program and attempt sporulation under starvation conditions, bypassing the requirement of mating-type heterozygosity (4). Although this mRNA modification in yeast is exclusively meiotic, and its dependency on Ime4 has been determined (5), the function of this modification in yeast meiosis remains unknown (6).

Our current knowledge of the biological function of *IME4* homologs in multicellular organisms is extremely limited, because mutants that compromise N^6-adenosine methyltransferase activity have not been described in any metazoan. In *Arabidopsis thaliana*, the *IME4* homolog, *MTA*, has been shown to be an essential gene, but its role in development has not been explored (7). The existence of a *Drosophila* homolog of *IME4* (CG5933) was reported in a comprehensive phylogenetic study of the evolution of methyltransferases (8). There exists a high degree of sequence similarity and conservation of the catalytic core among all eukaryotic homologs of *IME4* (5). Given the high degree of evolutionary conservation of *IME4* and its crucial function in the developmental decision of yeast to enter gametogenesis, we tested the hypothesis that *IME4* has a conserved function important for metazoan gametogenesis, focusing on oogenesis.

Drosophila oogenesis is a powerful system to identify gene functions controlling complex developmental events and signaling networks that are conserved in humans. The production of a fertilizable egg requires successive rounds of symmetry-breaking events that shape the follicle (egg chamber) and consequently define the future axes (polarity) of the embryo, as reviewed in ref. 9. Within the developmental unit of the fly ovary, the ovarioles, egg chambers composed of a germ-line cyst of 16 sister cells (15 nurse cells and one oocyte) encapsulated by a single layer of somatic follicle cells, emerge from the germarium and mature progressively. Egg-chamber maturation relies on continuous signaling between soma and germ line that drives morphogenetic processes and cell-fate determinations. Distinct follicle-cell fates are established early in oogenesis, specifically in germaria via Notch signaling, and are crucial for organizing the structure of the egg chamber, as reviewed in ref. 10.

Here we show that the *Drosophila* gene *Dm ime4* is essential for development, not solely for gametogenesis. We define a crucial role for the *Drosophila* gene in oogenesis. Our results indicate that Dm IME4 is required during oogenesis for processes that are regulated by Notch signaling and that involve soma–germ-line interactions. We provide an experimental paradigm to investigate the plausible evolutionary conservation of IME4 in metazoans as a model for the function of the human gene.

Results

***Dm ime4* Is Essential and Required for Fertility.** Using the Model Organisms Best Hits search engine (11), we found that the *Dm ime4* predicted protein (CG5933) shares significant amino acid similarity with its homologs in *S. cerevisiae* (*IME4*), *A. thaliana* (*MTA*), *Mus musculus* (*METTL3*), and *Homo sapiens* (*MT-A70*), all of which are known or predicted to function as mRNA methyltransferases (Fig. S1*A*). The core catalytic domain is highly conserved among species, and its presence is a reliable predictor of enzymatic function (Fig. S1*A*) (5, 12).

To define the function of *Dm ime4*, we generated deletions by P-element excision mutagenesis (13). Deletions that removed the *Dm ime4* gene were homozygous lethal (Fig. 1*A*). Two small deletions 5′ to *Dm ime4* (Fig. S1*B*) reduced expression of the gene and were semilethal (we could recover viable adults, albeit at much lower than expected Mendelian frequencies) (Fig. 1*B*, Fig. S2, and Table S1). The homozygous animals died in larval and pupal stages (*SI Materials and Methods*). The rare adults

Author contributions: C.F.H. and T.L.O.-W. designed research; C.F.H. performed research; C.F.H. and T.L.O.-W. analyzed data; and C.F.H. and T.L.O.-W. wrote the paper.

The authors declare no conflict of interest.

Freely available online through the PNAS open access option.

[1]To whom correspondence should be addressed. E-mail: weaver@wi.mit.edu.

This article contains supporting information online at www.pnas.org/lookup/suppl/doi:10.1073/pnas.1111577108/-/DCSupplemental.

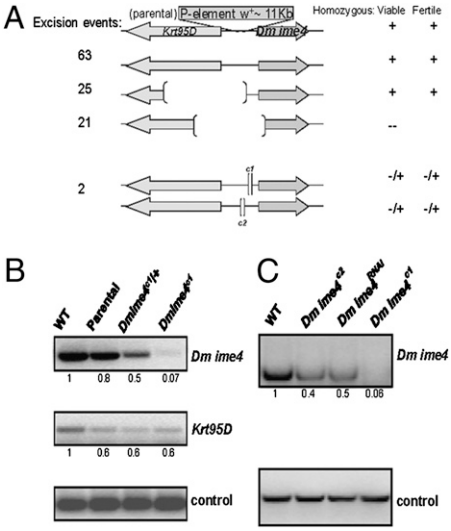

Fig. 1. *Dm ime4* is essential for viability. (*A*) P-excision mutagenesis events that deleted the *Dm ime4* ORF, partially or in its entirety, did not yield homozygous adult flies. Deletions of the adjacent *Krt95D* gene are viable. The small deletions 5′ to the *Dm ime4* gene greatly reduced female and male fertility. (*B*) The 5′ deletion in the *Dm ime4*^{c1} (shown) specifically affects mRNA levels of *Dm ime4* and does not affect mRNA levels of *Krt95D*. Transcript levels from whole flies were analyzed by RT-PCR in relation to a wild-type *Oregon R* control (numbers indicate relative abundance after quantification). Parental is the original P-element strain before P-element excision. *Dm ime4*^{c1}/+ is the heterozygous sibling balanced with *TM3*. *Dm ime4*^{c1} is the homozygous sibling rarely produced in the balanced stock. (*C*) Knockdown of *Dm ime4* via RNAi. *pUAST*-based RNAi lines (VDRC) were used to knock down *Dm ime4* using the ubiquitous *act5C-GAL4* driver. mRNA from whole adult flies was analyzed as in *B*. The strongest phenotypes were observed with the homozygous *Dm ime4*^{c1} allele, which resulted in significantly lower levels of *Dm ime4* than in the *Dm ime4*^{c2} allele or the *Dm ime4*^{RNAi} knockdown (Fig. S2).

recovered had significantly reduced fecundity. The severity of the semilethality and subfertility phenotypes correlated with decreased levels of *Dm ime4* (Fig. 1 *B* and *C* and Fig. S2); i.e., the effects of the *Dm ime4*^{c1} allele were more severe than those of the *Dm ime4*^{c2} allele.

As an independent means to confirm the phenotype, we inhibited *Dm ime4* by RNA interference with transgenic lines obtained from the Vienna Drosophila RNAi Center (VDRC) that have no predicted or reported off-targets (14). By inducing double-stranded RNA homologous to *Dm ime4* under *actin 5c-GAL4* control to ablate gene function throughout development (Fig.1*C* and Fig. S2), the semilethality and reduced fertility phenotypes were reproduced. The effectiveness of reducing *Dm ime4* levels via RNAi was comparable to the decrease in mRNA levels observed in *Dm ime4*^{c2} homozygous mutants (Fig. 1*C* and Fig. S2).

To verify that the mutant phenotypes were caused by mutation of the *Dm ime4* gene, we generated transgenic lines that expressed the *Dm ime4* gene or a mutant variant using the *GAL4- UAS* inducible system for phenotypic complementation of *Dm ime4*^{c1} homozygous mutants. The semilethality of the *Dm ime4*^{c1} mutant was rescued by expressing the *Dm ime4* gene under *UAS* control via *actin 5C-GAL4*, in that the recovery frequency of homozygous adults was equivalent to the expected Mendelian frequency for the cross (Table S1). In addition, the egg chamber phenotype described later in this report (see Fig. S6) also was rescued, and adults were fertile. Conversely, the semilethality of the *Dm ime4*^{c1} mutation was not rescued by expressing the *Dm ime4* gene harboring two point mutations in the conserved catalytic core under *UAS* control via *actin 5C-GAL*, despite the presence of mutant protein levels comparable to the wild type (Fig. S3). The recovery frequency of homozygous adults carrying the induced mutant transgene was equivalent to the frequency of the homozygous mutant without the induced transgene (Table S1). These point mutations are equivalent to the ones that result in loss of function in the *S. cerevisiae* homolog (5) and indicate conservation of the catalytic function of IME4 in *Drosophila*. In sum, our mutagenesis approach revealed an essential function for *Dm ime4* and allowed the recovery of hypomorphic mutations that permitted us to investigate its role in adult flies.

***Dm ime4* Is Expressed in Gonads.** To test the hypothesis that *Dm ime4* is required for gametogenesis, we assessed its mRNA levels in ovaries and testes of adult flies. *Dm ime4* was expressed in adult ovaries and testes but was not detectable in the carcasses from which gonads had been removed (Fig. 2 *A* and *B*). Our results were corroborated by cross-referencing the FlyAtlas gene expression database, where, as determined by microarray analysis, *Dm ime4* transcript levels in the adult were highest in gonads and were undetectable elsewhere (15). By in situ hybridization to ovaries, *Dm ime4* transcripts were detected in germaria, and hybridization signals persisted in later stages, when they were strongest in follicle cells (Fig. S4*A*). We chose to delineate the role of Dm IME4 in oogenesis because of the strong and specific expression of *Dm ime4* in adult ovary. Moreover, we could recover homozygous mutant adults, albeit at very low frequencies, and these adults had significantly reduced fecundity. Furthermore, in *Drosophila* oogenesis the mechanisms of meiosis parallel those in most metazoans, and the developmental regulatory events are well defined.

Dm IME4 Localizes to Soma and Germ-line Cells in Ovarioles. We generated polyclonal antibodies against Dm IME4 to investigate protein levels and protein distribution in ovaries. Dm IME4 protein was detected in ovaries and not in protein extracts from carcasses after ovary removal (Fig. 2*C*). Consistent with reduced mRNA levels of *Dm ime4* in *Dm ime4*^{c1} homozygotes, we observed significantly reduced levels of Dm IME4 protein compared with sibling heterozygous controls (Fig. 2*D* and Fig. S4*B*). By immunofluorescence, Dm IME4 was predominantly nuclear

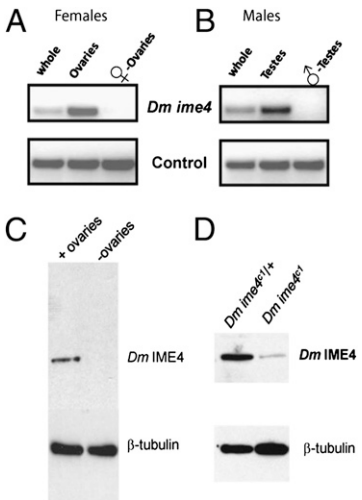

Fig. 2. *Dm ime4* is expressed in the gonads of adult flies. mRNA from whole flies, dissected gonads (ovaries or testes, as indicated), or carcasses without gonads was analyzed as in Fig. 1. (*A*) Adult females. (*B*) Adult males. (*C* and *D*) Western blot using Dm IME4 antisera. (*C*) Protein extracts from wild-type *Oregon R* whole flies or their remains after ovary removal showing that Dm IME4 protein can be detected only in whole flies and not in those devoid of ovaries. (*D*) Protein extracts from ovaries isolated from females of the indicated genotype showing significantly reduced levels of Dm IME4 in homozygous mutant flies.

(Fig. 3 *B–E*), consistent with its function in posttranscriptional modification of mRNA and similar to the human homolog, MT-A70, which localizes to nuclei of HeLa cells (2). Dm IME4 was detected in somatic (prefollicle, follicle, and polar) cells and in germ line-derived cells (Fig. 3*B*). Dm IME4 protein levels were strong in the middle region of germaria (asterisks in Fig. 3*B′*), which is the region where 16-cell cysts of sister germ cells begin to be surrounded by a single layer of somatic follicle cells to form the emerging egg chamber (16). In later egg chambers throughout oogenesis, Dm IME4 protein was observed in all follicle cells but particularly strongly in polar cells (asterisks in Fig. 3 *C′* and *D′*). Dm IME4 protein also could be detected in the ooplasm (arrow in Fig. 3*E′*) and in the cells of the 16-cell cyst of early stages (arrow in Fig. 3*B′*). These patterns of expression indicated a likely role in egg chamber development, as addressed below.

***Dm* IME4 Is Required for Egg Chamber Development.** Motivated by the protein-localization pattern of Dm IME4 throughout oogenesis in wild-type ovarioles and the decreased fecundity of *Dm ime4* homozygous mutants, we predicted a role for Dm IME4 in oogenesis. To verify this prediction, we analyzed the morphology of ovarioles from homozygous mutants. The most significant and penetrant early phenotype was compound egg chambers with supernumerary nurse cells in the ovaries of the rare *Dm ime4*^{c1} homozygous mutant adults. This phenotype was observed in up to 70% of the mutant ovarioles examined (arrow in Fig. 4*A′* and Table S2). Mutant ovarioles that contained a significant number of compound egg chambers rarely matured past midoogenesis; egg chambers at later stages frequently were degenerating with pyknotic nuclei (asterisk in Fig. 4*A′*). Even in the absence of detectable compound egg chambers, seemingly normal ovarioles in the mutants also displayed a high frequency of degenerating egg chambers, and only 10% had mature egg chambers in vitellogenic stages (Table S2). Using an independent experimental approach, we also observed the compound egg chamber phenotype following heat-shock GAL4-induced *Dm ime4* RNAi in females (Fig. S5). Finally, the mutant phenotype is caused by the *Dm ime4* mutation, because the *Dm ime4* wild-type transgene can rescue the compound follicle phenotype of the mutants (Fig. S6).

We first addressed the nature of the germ cells in compound egg chambers. By labeling with the oocyte marker, Orb, we found that the mutant follicles contained two or more oocytes that failed to localize to the posterior end (arrowheads in Fig. 4*B′*). To determine whether the supernumerary germ cells originated from extra rounds of mitosis, we used an antibody that localizes to the cytoplasmic bridges (ring canals) between the oocyte and its sister nurse cells. In a normal 16-cell cyst there are four ring canals between the oocyte and its sister cells (Fig. 4*C*). We found that, with few exceptions (Fig. 4 *C′′*), nearly all oocytes in compound follicles were surrounded by four ring canals; thus the majority of the cysts originated from the normal four rounds of mitotic divisions before entry of the oocyte into meiosis (Fig. 4*C′* and Table S2). In addition, the number of nurse cells in the compound follicles usually corresponded to a multiple of the number of oocytes detected; e.g., if three oocytes were detected, 45 nurse cells were present in that egg chamber.

We next investigated whether these oocytes in compound follicles entered meiosis by using an antibody against the central protein in the synaptonemal complex, C(3)G (Fig. 4 *D* and *D′*). We observed synaptonemal complex formation in these oocytes (Fig. 4 *D′*), indicating they entered meiosis.

Given that the compound follicles appeared to result primarily from the encapsulation of several 16-cell cysts into a common egg chamber, we examined follicle-cell morphology in the mutants. To trace the earliest signs of compound egg-chamber formation, we looked at the germaria of *Dm ime4*^{c1} mutants. A common feature of mutant germaria is the presence of two, sometimes more, partially encapsulated germ-line cysts located on the same plane (Fig. 5*A′*), instead of a single cyst file formed upon encapsulation as seen in the control germaria (Fig. 5*A*). In egg chambers that emerged from the germaria, we observed that follicle cells were disorganized and that specialized follicle-cell types, such as polar cells, frequently were absent or mislocalized (Fig. 5*B′*). Stalks (i.e., the cells that separate these follicles) were wider than normal stalks or were missing completely (Fig. 5 *C* and *C′*). In the most severe cases, there was a continuum of germ-line cysts from germaria to subsequent maturing stages (as discernable by the size of nurse cell nuclei; asterisk in Fig. 5*A′*) with no apparent cyst individualization (arrow in Fig. 5*A′* and Table S2). Normally, Fasciclin III is down-regulated in epithelial follicle cells after

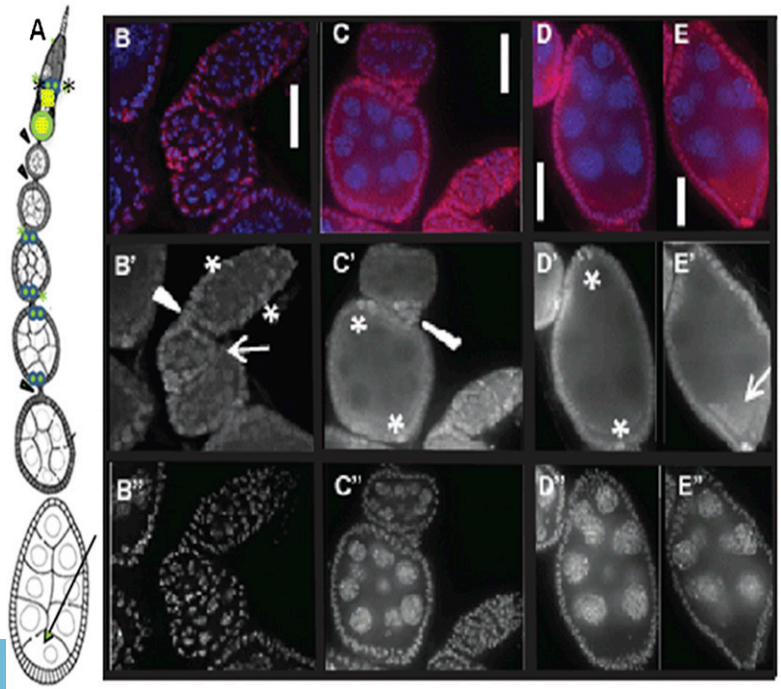

Fig. 3. Dm IME4 is abundant in follicle cells and also is detectable in early germ-line cysts. (*A*) Diagram of a *Drosophila* ovariole in the anterior–posterior orientation, with the germarium at the top. Asterisks at the middle of the germarium show the location of prefollicle cells (marked with asterisks in *B′*). Arrowheads show stalk cells connecting the egg chambers. Twin green dots marked with green asterisks show the location of anterior and posterior polar cells (marked with asterisks in *C′* and *D′*). Arrow shows the location of the ooplasm (arrow in *E′*). (*B–E*) Distribution of Dm IME4 protein (red) in ovarioles, showing localization in follicle cells and in germ-line cells. Panels are oriented so that top is anterior and bottom is posterior, as depicted in the cartoon in *A*. DAPI staining is blue. (*B′–E′*) Dm IME4 single channel. (*B′′–E′′*) DAPI single channel. (*B–B′′*) Distribution of Dm IME4 protein in germaria showing prefollicle cells (asterisks in *B′*), stalk (arrowhead in *B′*), and early egg chambers (stages 2 and 3) where Dm IME4 is abundant in follicle and less abundant but reproducibly observed in germ-line cyst cells (arrow in *B′*). (*C–C′′*) Germaria and stages 4 and 5, localization of Dm IME4 in stalk (arrowhead in *C′*) and polar cells (asterisks in *C′*). (*D–D′′*) Stage 7, localization of Dm IME4 in all follicle cells and abundantly in polar cells (asterisks in *D′*) and forming a crescent shape (ooplasm). (*E*) Stage 8, localization of Dm IME4 in follicle cells, polar cells, and abundantly in ooplasm (arrow in *E′*). (Scale bars: 10 μm.)

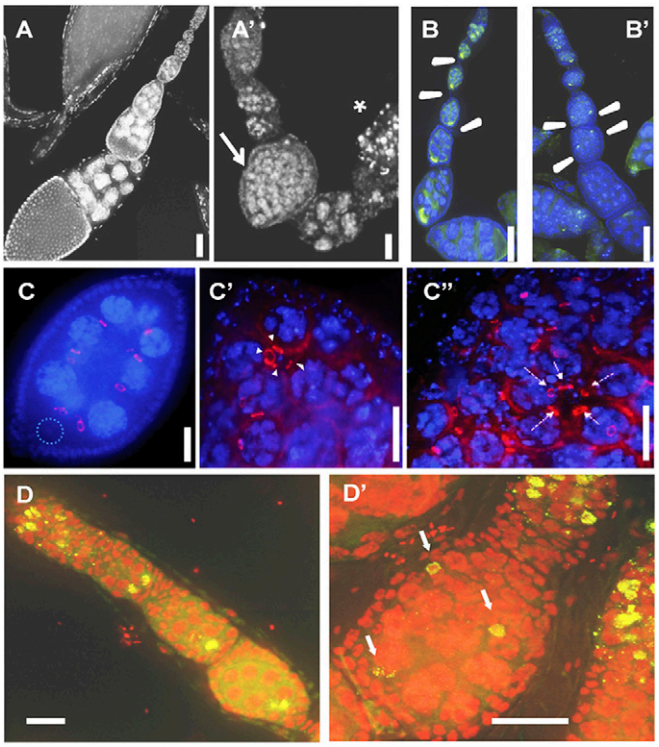

Fig. 4. Oogenesis defects in *Dm ime4* mutants. All images are oriented with anterior at the top. (*A*, *B*, *C*, and *D*) *Dm ime4*^{c1}/+ control. (*A′*, *B′*, *C′*, *C″*, and *D′*) *Dm ime4*^{c1} homozygous. (*A* and *A′*) DAPI nuclear staining showing a representative example of the control (*A*) and a *Dm ime4*^{c1} mutant ovariole (*A′*) with a compound follicle (arrow in *A′*) and a degenerating previtellogenic egg chamber (asterisk in *A′*) (Refer to Table S2 for quantification of these phenotypes). (*B* and *B′*) Compound follicles in *Dm ime4*^{c1} mutants have multiple oocytes [indicated by green Orb staining (arrowheads)] that fail to localize to the posterior end of the follicle. (*C* –*C″*) Most compound egg chambers of *Dm ime4*^{c1} mutants have multiple 16-cell germ-line cysts (15 nurse cells and one oocyte) from four rounds of mitosis, as indicated by the presence of four ring canals visualized by Kelch antibody (arrowheads in *C′*) surrounded by a common layer of follicle cells. Dotted circle in *C* shows position of the posteriorly located oocyte. Five ring canals (arrows in *C″*) can be seen around the oocyte at low frequency. (*D* and *D′*) Oocytes in *Dm ime4*^{c1} compound follicles entered meiosis and assembled the synaptonemal complex (arrows in *D′*) as visualized by C(3)G antibody (green). DNA was detected with propidium iodide (red). (Scale bars: 10 μm.)

stage 2, remaining at high levels in later stages solely in polar cells (17). In contrast, this down-regulation of Fasciclin III was rarely observed in *Dm ime*^{c1} mutant follicles (Fig. 5*B′*). Taken together, our results show severe defects in egg-chamber encapsulation and follicle-cell differentiation in *Dm ime4* homozygous mutants that resembled defects in signaling between soma and germ line (18).

Notch Signaling Is Reduced in *Dm ime4* Mutant Follicle Cells. Defects in cyst encapsulation resulting in compound follicles and previtellogenic egg-chamber degeneration, the major phenotypes of *Dm ime4* mutant ovaries, also are observed in mutants that affect Notch signaling: Delta, Notch itself, or Presenilin mutants (19). Therefore, we tested whether Notch signaling was compromised in *Dm ime4* mutant ovarioles by using a transgenic line that permits visualization of Notch activation via a reporter fused to the Suppressor of Hairless regulatory region (20). The rare viable *Dm ime4*^{c1} homozygous adults with this reporter showed a significant decrease in the levels and in the number of follicle cells positive for Notch activation (Fig. 6 *B* and *B′*) compared with heterozygous siblings (arrows in Fig. 6 *A* and *A′*), implying that Dm IME4 is required for Notch signaling in oogenesis.

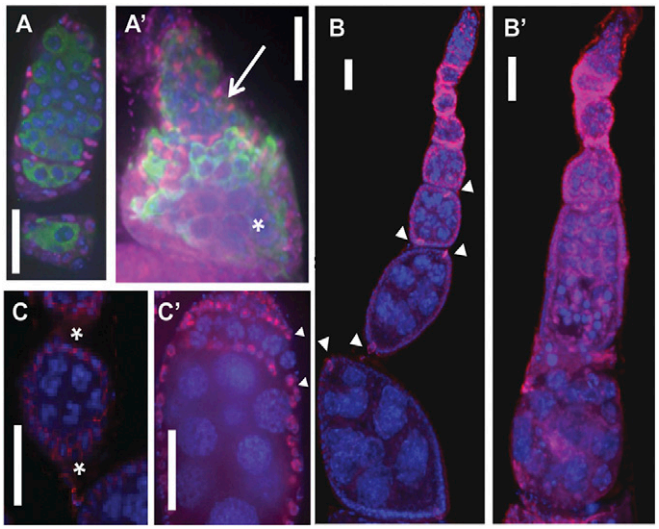

Fig. 5. Defects in cyst encapsulation and follicle-cell specification in *Dm ime4* mutants. (*A*) Control germarium. (*A′*) Representative germarium of a *Dm ime4* homozygote in which cysts fail to follow an orderly pattern as they progress and have incomplete follicle-cell encapsulation (arrow). These trapped germ-line cysts can progress through other developmental stages, as shown by the increased size of the nurse cells at the bottom of this compound germarium (asterisk). Follicle cells were visualized with Traffic Jam (TJ, red). Germ-line cysts were visualized with *VASA* antibody staining (green). All nuclei were stained with DAPI (blue). (*B* and *B′*) Polar cells indicated by arrowheads in control *Dm ime4*^{c1} /+ follicles (*B*) are aberrant or missing in *Dm ime4*^{c1} compound follicles (*B′*). (*C* and *C′*) Stalks seen in control *Dm ime4*^{c1} /+ (asterisks in *C*) frequently are missing in *Dm ime4*^{c1} homozygous mutants (*C′*), and egg chambers pack atop of each other. (Arrowheads in *C′* mark the developmental stage shown between the asterisks in *C*.) FasIII staining is, red; DAPI staining is blue. (Scale bars: 10 μm.)

Expression of Notch^{ICD} Rescues the Compound Egg Chamber Phenotype in *Dm ime4* Mutant Ovaries. Because we observed a significant decrease in Notch signaling in the *Dm ime4* mutant follicle cells, we tested whether expression of a constitutively activated form of Notch (Notch^{ICD}, IntraCellular Domain) could suppress the ovarian phenotypes in *Dm ime4* mutants. Overexpression of Notch^{ICD} is deleterious before adulthood; thus Notch^{ICD} was induced under the control of the heat-shock promoter *Hsp70* in females only after eclosion by performing daily heat-shock treatments for 5 d before dissection. An important aspect of egg-chamber formation is that somatic follicle-cell differentiation is coordinated with germ-line events by cell–cell communication via Notch signaling. Disruption in soma–germ line communication leads to formation of aberrant egg chambers that frequently degenerate in previtellogenic stages and are not ovulated. As shown in Fig. 7, expression of Notch^{ICD} significantly reduced the frequency of compound egg-chamber formation in *Dm ime4* mutant ovaries and allowed progression through oogenesis past the previtellogenic stages. The other significant phenotype of *Dm ime4* mutant ovaries is the high frequency of degenerating egg chambers, but the suppression of this phenotype cannot be assessed accurately because of the high incidence of pyknotic nuclei that arise even in the controls during heat-shock treatment (Fig. 7). Of note, we observed significant suppression of the *Dm ime4* mutant phenotypes in the ovaries of females that carried the Notch^{ICD} transgene even in the absence of heat-shock treatment, probably because of leaky activity of the *Hsp70* promoter at room temperature (21).

Discussion

Here we describe the role of the Dm IME4 mRNA N^6-adenosine methyltransferase in the development of a metazoan organism. We find that, in contrast to the homologous gene in the unicel-

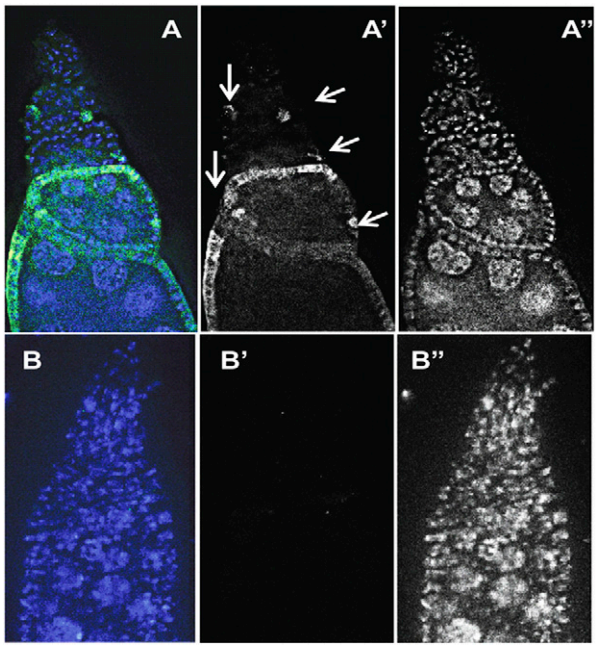

Fig. 6. Notch signaling is reduced in *Dm ime4* mutants. (*A* and *A′*) Notch signaling as detected in *Gbe+ Su(H)-lacZ/FM7*; *Dm ime4*^{c1}*/TM6b* control (arrows indicate sites of Notch activity detected in the control). (*B* and *B′*) *Gbe+ Su(H)-lacZ/FM7*; *Dm ime4*^{c1} mutants have significantly lower levels of Notch activity than the sibling *Gbe+ Su(H)-lacZ/FM7*; *Dm ime4*^{c1}*/TM6b* controls as visualized by anti–β-galactosidase staining (green). *A* and *B* show merged anti–β-galactosidase (green) and DAPI (blue) channels; *A′* and *B′* show an anti–β-galactosidase (green) single channel. *A″* and *B″* show a DAPI single channel (white).

lular eukaryote *S. cerevisiae*, *Dm ime4* is an essential gene. In adults, we show that Dm IME4 is required for male and female fertility. In females, Dm IME4 is essential for oogenesis, and loss of function shows defects consistent with failure in soma–germ line interactions. We find that Notch signaling is reduced in *Dm ime4* mutants, suggesting a function for Dm IME4 in the Notch signaling pathway. Furthermore, Dm IME4 probably functions upstream of this signaling pathway, because the expression of a constitutively activated form of Notch rescues the compound egg chamber phenotype of *Dm ime4* homozygous females.

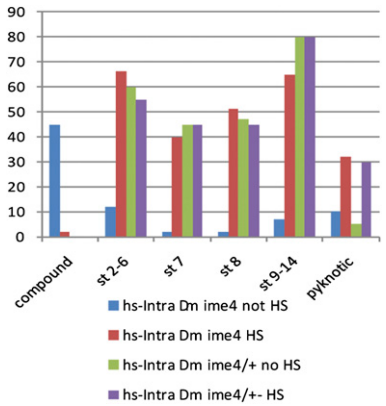

Fig. 7. Notch^{ICD} rescues egg-chamber defects in *Dm ime4* mutants. Bar graph shows quantification of 100 ovarioles for each of the genotypes and conditions assayed as described in the graph color key. Lines carrying the heat shock-inducible Notch^{ICD} construct are designated as hs-Intra, heat-shocked treated (HS), or not treated (no HS). Egg chambers in 100 ovarioles were scored and are represented on the *x* axis as follows: compound egg chambers (compound); previtellogenic stages 2–6 (st 2–6) and stage 7 (st 7); vitellogenic stage 8 (st 8) and stages 9–14 (st 9–14); and degenerating egg chambers (pyknotic).

The essential function of *Dm ime4* probably is a common feature in multicellular organisms. In *A. thaliana*, *MTA*, the *Dm ime4* homolog, is essential for embryogenesis, because loss-of-function homozygous mutants are unable to proceed through embryogenesis past the globular stage and thus are unable to form differentiated tissues (7). Although the focus of this report is the function of Dm IME4 in oogenesis, homozygous mutant males also have reduced fertility; thus it will be interesting to determine the function of *Dm ime4* in spermatogenesis and uncover similarities or differences in the roles of Dm IME4 in the ovary and testis. Further investigation of Dm IME4 function before its role in adult gametogenesis will reveal whether the protein controls cell differentiation in a variety of developmental contexts. Interestingly, the rare *Dm ime4* mutant adults that are obtained have a high incidence of Notched wings, raising the possibility that Dm IME4 is required for Notch signaling in other developmental stages and tissues.

The defects in oogenesis that we observe when *Dm ime4* function is compromised can be explained by failure of Notch signaling in follicle cells starting early in the germaria. *Dm ime4* mutants and *Dm ime4* ablation via RNAi show defects in germ line–soma interactions leading to failure of follicle-cell differentiation, as shown by absence of stalks and polar cells and aberrant germ-line cyst encapsulation, similar to defects previously reported for Notch signaling mutants (19). Defects in soma–germ-line communication, like those described for Notch signaling mutants, lead to the formation of aberrant egg chambers, which are eliminated via apoptosis (22). In addition to the phenotypic similarities between *Dm ime4* and Notch signaling mutants, we observed significantly lower Notch reporter activity in *Dm ime4* mutants than in sibling controls, indicating that Notch signaling is compromised by low levels of Dm IME4. Because the oogenesis phenotype of *Dm ime4* homozygous mutants can be rescued fully by expressing an activated form of Notch, we show that Notch signaling is the pathway primarily affected in oogenesis in *Dm ime4* mutants. Taken together, our data indicate that Dm IME4 is a key player in Notch signaling, probably functioning upstream of Notch activation. It will be interesting to determine how the enzymatic function of Dm IME4 affects this signaling pathway and whether transcripts harboring N^6-mA–modified mRNA are involved in Notch signaling during soma–germ line interactions.

The function of yeast IME4 is to allow entry into meiosis; thus we expected a defect in meiotic entry in *Dm ime4* mutants. Because a complete deletion of *Dm ime4* is lethal, we could not investigate the phenotypic consequences of total absence of Dm IME4 protein in oogenesis. With this caveat, *Dm ime4* mutants that cause reduced fertility and ovary degeneration do not affect the onset of meiosis, as we can detect synaptonemal complex assembly in the oocytes of mutant egg chambers.

The protein expression of Dm IME4 and the phenotypes indicate a requirement in both the soma and the germ line. The mutant phenotype of compound egg chambers is caused by the inability of follicle cells to encapsulate a single 16-cell germ-line cyst, suggesting that the major role of Dm IME4 in oogenesis is in the somatic follicle cells. It is possible, however, that soma and germ line have different threshold requirements for Dm IME4 protein levels, and the reduction of Dm IME4 in the hypomorphic alleles may have affected the follicle cells primarily. We observed, albeit at low frequency, an extra round of mitotic germ-line cyst divisions. This phenotype is a consequence of Dm IME4 acting in the germ line, because it can be reproduced by RNAi knockdowns using germ-line drivers (Fig. S5). Taken together, our results suggest that Dm IME4 acts in both germ line and soma and plays a role in signaling between these two lineages during gametogenesis. In follicle cells this signaling appears to be accomplished via the Notch pathway.

In yeast, *IME4* controls a crucial developmental decision in this unicellular eukaryote's life cycle: to continue mitosis or to enter the gametogenesis program (4). The present demonstration of developmental functions of *Drosophila* IME4 shows how a conserved function can be expanded in evolution, in this case for use in multiple developmental decisions and to target a signal transduction pathway that does not exist in yeast (23).

Materials and Methods

Ethics Statement. The protocol for production of polyclonal antibodies against Dm IME4 was reviewed and approved by the Committee for Animal Care of the Massachusetts Institute of Technology.

Strains and Genetic Manipulations. Bloomington strain *13927: y^1; ry^{506} P{SUPor-P}KrT95D^{KG02054}* harboring a P-element insertion marked with *white*$^+$ in the intergenic region between *Dm ime4* (CG5933) and Krueppel target at 95D (*Krt95D*) was used to induce P-element excision events via transposase to delete *Dm ime4*. The inducible *Dm ime4* and catalytic domain mutant rescue constructs were generated by cloning the entire *Dm ime4* cDNA in a *pUASP*-based Gateway vector as described (24), and their expression was induced by *Actin5C-GAL4*. Transgenic flies were provided by BestGene, Inc. The *Gbe*$^+$ *su(H)-lacZ/FM7; TM2/TM6* transgenic line used to visualize Notch activity was provided by Sara Bray (University of Cambridge, Cambridge, UK) (25). The *Hsp70-*Notch^{ICD} transgenic line used to induce activated Notch by heat-shock treatment was a gift from Toby Lieber (Rockefeller University, New York, NY) (26).

Gene Expression. Transcript levels were quantified by RT-PCR. In situ hybridization was performed as previously described (27).

Antibody Generation and Protein Detection. Antigens and antibodies were generated as previously described (28). IME4 antigens were generated as GST-fusions of 0.8-kb and 1.2-kb fragments of *Dm ime4* cDNA with high scores by antigenicity algorithm (29) and no predicted cross-reactivity. Anti-Dm IME4 antiserum was produced in guinea pigs (Covance, Inc). Western blots were performed as described (30).

Immunofluorescence. Ovaries were dissected from 1- to 3-d-old females and fixed as previously described (31), with modifications given in *SI Materials and Methods*. All antibody dilutions were vol/vol. Dm IME4 antiserum from guinea pig was used at 1:1,000 dilution; mouse Fasciclin III (Developmental Studies Hybridoma Bank, DSHB) was used at 1:50; mouse Orb (DSHB) at 1:50 was amplified with anti-mouse biotin and visualized with FITC-streptavidin; mouse Kelch and mouse anti–Hts-RC (DSHB) at were used at 1:50; mouse C(3)G (a gift from Scott Hawley, Stowers Institute, Kansas City, MO) was used at 1:2,000, and samples for C(3)G detection were prepared as previously described (32). Guinea pig anti-Traffic Jam (a gift from Dorothea Godt, University of Toronto, Toronto, ON, Canada) was used at 1:5,000; rabbit anti-VASA (a gift from Ruth Lehmann, Skirball Institute, New York, NY) was used at 1:2,000; and anti–β-galactosidase (40-1a) (DSHB) was used at 1:50. Incubations with corresponding secondary fluorescent antibodies were done in PBS/3% BSA/0.1% Triton-X for 1 h at room temperature, at a dilution of 1:500. DAPI staining was done last, using a concentration of 1 μg/mL in PBS/0.5%BSA. Ovaries were mounted with VECTASHIELD (Vector Labs) or Aqua Poly/Mount (PolySciences) on polylysine-coated slides to immobilize ovaries for *z*-stack acquisition. Microscopic observations and imaging were done using a Nikon Eclipse Ti Epifluorescent inverted microscope with 10× and 20× dry objectives or 60× and 100× oil-immersion objectives, and images were analyzed using Nikon's NIS-Elements software.

ACKNOWLEDGMENTS. We thank Gerald R. Fink for encouragement and support in undertaking this project, fruitful discussions throughout the development of this work, and critical reading of the manuscript. Peter Reddien, Mark Gill, Jessica Chang, and Belinda Pinto provided insightful comments on the manuscript. We thank Sara Bray and Todd Nystul for the Notch activation reporter lines; Toby Lieber for the Hsp70-Notch^{ICD} line; and Mary Lilly, Dorothea Godt, Ruth Lehmann, and Scott Hawley for antibodies. The Bloomington Stock Center and VDRC provided stocks and Flybase genetic information. This work was supported by a National Institutes of Health K99 Pathways to Independence award and National Institutes of Health American Recovery and Reinvestment Act funds (to C.F.H.) and an American Cancer Society Research Professor Grant (to T.L.O.-W.).

1. Narayan P, Rottman FM (1992) Methylation of mRNA. *Adv Enzymol Relat Areas Mol Biol* 65:255–285.
2. Bokar JA, Shambaugh ME, Polayes D, Matera AG, Rottman FM (1997) Purification and cDNA cloning of the AdoMet-binding subunit of the human mRNA (N6-adenosine)-methyltransferase. *RNA* 3:1233–1247.
3. Shah JC, Clancy MJ (1992) IME4, a gene that mediates MAT and nutritional control of meiosis in *Saccharomyces cerevisiae*. *Mol Cell Biol* 12:1078–1086.
4. Hongay CF, Grisafi PL, Galitski T, Fink GR (2006) Antisense transcription controls cell fate in *Saccharomyces cerevisiae*. *Cell* 127:735–745.
5. Clancy MJ, Shambaugh ME, Timpte CS, Bokar JA (2002) Induction of sporulation in Saccharomyces cerevisiae leads to the formation of N6-methyladenosine in mRNA: A potential mechanism for the activity of the IME4 gene. *Nucleic Acids Res* 30: 4509–4518.
6. Bodi Z, Button JD, Grierson D, Fray RG (2010) Yeast targets for mRNA methylation. *Nucleic Acids Res* 38:5327–5335.
7. Zhong S, et al. (2008) MTA is an Arabidopsis messenger RNA adenosine methylase and interacts with a homolog of a sex-specific splicing factor. *Plant Cell* 20:1278–1288.
8. Bujnicki JM, Feder M, Radlinska M, Blumenthal RM (2002) Structure prediction and phylogenetic analysis of a functionally diverse family of proteins homologous to the MT-A70 subunit of the human mRNA:m(6)A methyltransferase. *J Mol Evol* 55: 431–444.
9. Roth S, Lynch JA (2009) Symmetry breaking during Drosophila oogenesis. *Cold Spring Harb Perspect Biol* 1:a001891.
10. Huynh JR, St Johnston D (2004) The origin of asymmetry: Early polarisation of the Drosophila germline cyst and oocyte. *Curr Biol* 14:R438–R449.
11. Balakrishnan R, et al. (2005) Fungal BLAST and Model Organism BLASTP Best Hits: New comparison resources at the Saccharomyces Genome Database (SGD). *Nucleic Acids Res* 33(Database issue):D374–D377.
12. Bokar JA, Rath-Shambaugh ME, Ludwiczak R, Narayan P, Rottman F (1994) Characterization and partial purification of mRNA N6-adenosine methyltransferase from HeLa cell nuclei. Internal mRNA methylation requires a multisubunit complex. *J Biol Chem* 269:17697–17704.
13. Engels WR, Johnson-Schlitz DM, Eggleston WB, Sved J (1990) High-frequency P element loss in Drosophila is homolog dependent. *Cell* 62:515–525.
14. Dietzl G, et al. (2007) A genome-wide transgenic RNAi library for conditional gene inactivation in Drosophila. *Nature* 448:151–156.
15. Chintapalli VR, Wang J, Dow JA (2007) Using FlyAtlas to identify better *Drosophila melanogaster* models of human disease. *Nat Genet* 39:715–720.
16. Margolis J, Spradling A (1995) Identification and behavior of epithelial stem cells in the Drosophila ovary. *Development* 121:3797–3807.
17. Wu X, Tanwar PS, Raftery LA (2008) Drosophila follicle cells: Morphogenesis in an eggshell. *Semin Cell Dev Biol* 19:271–282.
18. Cummings CA, Cronmiller C (1994) The *daughterless* gene functions together with Notch and Delta in the control of ovarian follicle development in Drosophila. *Development* 120:381–394.
19. López-Schier H, St Johnston D (2001) Delta signaling from the germ line controls the proliferation and differentiation of the somatic follicle cells during Drosophila oogenesis. *Genes Dev* 15:1393–1405.
20. Furriols M, Bray S (2000) Dissecting the mechanisms of suppressor of hairless function. *Dev Biol* 227:520–532.
21. Lebedeva LA, et al. (2005) Occupancy of the Drosophila hsp70 promoter by a subset of basal transcription factors diminishes upon transcriptional activation. *Proc Natl Acad Sci USA* 102:18087–18092.
22. Buszczak M, Cooley L (2000) Eggs to die for: Cell death during Drosophila oogenesis. *Cell Death Differ* 7:1071–1074.
23. Gazave E, et al. (2009) Origin and evolution of the Notch signalling pathway: An overview from eukaryotic genomes. *BMC Evol Biol* 9:249.
24. Akbari OS, Oliver D, Eyer K, Pai CY (2009) An Entry/Gateway cloning system for general expression of genes with molecular tags in Drosophila melanogaster. *BMC Cell Biol* 10:8.
25. Furriols M, Bray S (2001) A model Notch response element detects Suppressor of Hairless-dependent molecular switch. *Curr Biol* 11:60–64.
26. Lieber T, Kidd S, Alcamo E, Corbin V, Young MW (1993) Antineurogenic phenotypes induced by truncated Notch proteins indicate a role in signal transduction and may point to a novel function for Notch in nuclei. *Genes Dev* 7:1949–1965.
27. Tzolovsky G, Deng WM, Schlitt T, Bownes M (1999) The function of the *broad-complex* during *Drosophila melanogaster* oogenesis. *Genetics* 153:1371–1383.
28. Moore DP, Page AW, Tang TT, Kerrebrock AW, Orr-Weaver TL (1998) The cohesion protein MEI-S332 localizes to condensed meiotic and mitotic centromeres until sister chromatids separate. *J Cell Biol* 140:1003–1012.
29. Hopp TP, Woods KR (1981) Prediction of protein antigenic determinants from amino acid sequences. *Proc Natl Acad Sci USA* 78:3824–3828.
30. Wolff T (2000) Histological techniques for the Drosophila eye part I: Larva and Pupa. *Drosophila Protocols*, eds Sullivan W, Ashburner M, Hawley RS (Cold Spring Harbor Laboratory Press, Cold Spring Harbor, NY), pp 207–212.
31. Resnick TD, et al. (2009) Mutations in the chromosomal passenger complex and the condensin complex differentially affect synaptonemal complex disassembly and metaphase I configuration in Drosophila female meiosis. *Genetics* 181:875–887.
32. Khetani RS, Bickel SE (2007) Regulation of meiotic cohesion and chromosome core morphogenesis during pachytene in Drosophila oocytes. *J Cell Sci* 120:3123–3137.